LBNL-42403
Preprint

ERNEST ORLANDO LAWRENCE BERKELEY NATIONAL LABORATORY

Thermodynamics and the Other Chemical Engineering Sciences: Old Models for New Chemical Processes

John M. Prausnitz

Chemical Sciences Division

October 1998

Submitted to
Fluid Phase Equilibria

REFERENCE COPY
Does Not
Circulate
Bldg. 50 Library - Ref.
Lawrence Berkeley National Laboratory

Copy 1

LBNL-42403

DISCLAIMER

This document was prepared as an account of work sponsored by the United States Government. While this document is believed to contain correct information, neither the United States Government nor any agency thereof, nor the Regents of the University of California, nor any of their employees, makes any warranty, express or implied, or assumes any legal responsibility for the accuracy, completeness, or usefulness of any information, apparatus, product, or process disclosed, or represents that its use would not infringe privately owned rights. Reference herein to any specific commercial product, process, or service by its trade name, trademark, manufacturer, or otherwise, does not necessarily constitute or imply its endorsement, recommendation, or favoring by the United States Government or any agency thereof, or the Regents of the University of California. The views and opinions of authors expressed herein do not necessarily state or reflect those of the United States Government or any agency thereof or the Regents of the University of California.

LBNL-42403

Thermodynamics and the Other Chemical Engineering Sciences: Old Models for New Chemical Processes

John M. Prausnitz
Department of Chemical Engineering
University of California
and
Chemical Sciences Division
Lawrence Berkeley National Laboratory
University of California
Berkeley, CA 94720, U.S.A.

October 1998

This work was supported by the Director, Office of Energy Research, Office of Basic Energy Sciences, Chemical Sciences Division of the U.S. Department of Energy under Contract Number DE-AC03-76SF00098.

Thermodynamics and the Other Chemical Engineering Sciences: Old Models for New Chemical Products and Processes

J. M. Prausnitz
Chemical Engineering Department
University of California, Berkeley
and
Chemical Sciences Division
Lawrence Berkeley National Laboratory
Berkeley, CA 94720 USA
E-mail:lindar@cchem.berkeley.edu

Much recent academic research in molecular thermodynamics has been directed toward ever-more-complex theories without adequate attention to how such theories may be used in contemporary chemical technology; too often, researchers develop theories for their own sake, delegating to others (who?) to figure out how to use them.

For new chemical product design, it is typically necessary to inter-relate thermodynamics with other sciences (notably mass transfer); for chemical process design, it is desirable to direct molecular-thermodynamic ideas toward evolving industries (e.g., biotechnology). Toward those ends, conventional models can often provide helpful information. To illustrate, three examples are briefly discussed: first, design of a drug-delivery system and second, design of polymer blends to achieve desired mechanical properties. In both examples, the key to success is not the conventional molecular model but its combination with Fickian diffusion.

The third example concerns precipitation of proteins from aqueous salt solutions; a remarkably simple model shows how equilibria in protein solutions are qualitatively different from those in conventional solutions. Calculations show that, for protein solutions, on a plot of temperature versus concentration, the freezing line (for liquid-solid equilibria) lies above the liquid-liquid coexistence curve, as verified by experiment.

Key words: Molecular Thermodynamics, Polymer Blends, Landau-Ginzburg Expansion, Drug-Delivery System, Fick's Law, Protein Solutions

Near the end of his life, about 50 years ago, Albert Einstein described the modern world with a striking remark:

"Our times are characterized by perfecting the means while confusing the goals."

Einstein's insight applies to many aspects of contemporary culture including, I think, much of chemical engineering thermodynamics, especially if we substitute "neglecting" for "confusing". Our best minds spend time and talent on developing ever more sophisticated theories with impressive results. But all too often, when I see these impressive results, I ask myself: What can I do with this? How does this help me as a chemical engineer? Frequently, I have no response.

Chemical engineering thermodynamics has many talented researchers working on a wide variety of projects. It is therefore not appropriate to generalize. But all too often when I read erudite articles in the literature, the author of the article seems to be saying: "I have an answer. But I don't know the question."

I represent an old-fashioned view: chemical engineering thermodynamics should be application-oriented and research in chemical engineering thermodynamics should be concerned with new applications. One area for new applications is to describe phase equilibria for unconventional mixtures, that is, those mixtures that are found in emerging chemical industry where so far, we do not have a satisfactory quantitative description. I shall briefly present an example later.

The second area concerns a new direction for chemical engineering

thermodynamics: product development. In the past, primary attention has been given to developing more efficient processes for producing standard chemical products. Historically, chemists established a product and the task of chemical engineering thermodynamics was to help design a cost-effective process for making that product in large quantities. That task is still with us but, as manufacture of commodity chemicals is becoming routine, a challenging and more promising task for chemical engineering thermodynamicists is to provide assistance in developing new chemical products. I want to show two examples that illustrate such assistance. One of these examples is over 20 years old and remarkably simple; the second, more recent example is more complex. Both examples illustrate two important features: first, thermodynamics can provide only a partial answer; for effective assistance to product development, thermodynamics must often be combined with rate phenomena, perhaps chemical kinetics or, as in my two examples, mass transfer. Second, the required theory is often quite old; it is remarkable, how old theories can frequently be applied to new problems. In my examples, emphasis is not on the theory, but on the method of applying the theory. These two examples illustrate the timeless advice of St. Augustine. Non nova sed nove (Not new, but in a new way).

Design of a Drug-Delivery System

When combined with elementary diffusion theory, chemical thermodynamics can contribute toward development of a new chemical product. An early illustration was provided in 1975 by Alan Michaels and co-workers at the Alza Corporation (in Palo Alto, California) who were concerned with the design of a new drug-delivery system (1).

Michaels showed that, to optimize the design, it was useful to correlate and interpret limited experimental flux data using the simple regular-solution theory of Hildebrand that dates back to about 1930.

Michaels was interested in constructing a contraceptive device that very slowly releases a powerful contraceptive drug inside the uterus. The drug, a steroid hormone, is placed inside a polymeric coating, as shown in Figure 1. The steroid diffuses slowly through the polymeric coating into the uterus. The important design parameter is the thickness of the polymer coating; that thickness is determined by the permeability of the drug in the polymer. The permeability is determined, in part, by the solubility of the drug in the polymer.

To optimize product design, Michaels considered a variety of steroids and polymers. To reduce experimental effort, he wanted to correlate limited flux data; he used some simple thermodynamics toward establishing that correlation.

The flux of drug A is given by

$$\hat{J}_A = \frac{D}{\ell}\,[C_A(0) - C_A(\ell)] \tag{1}$$

where ℓ is the thickness of the polymer coating and D is the diffusivity. $C_A(0)$ is the concentration of A at the inner wall and $C_A(\ell)$ is the concentration of A at the outer wall.

Because the fluid in the uterus washes away any molecule A that reaches the outside of the polymer wall,

$$C_A(\ell) = 0 \tag{1a}$$

At the inner wall, $C_A(0)$ is the saturation concentration because, at the inner wall,

steroid in the polymer is in equilibrium with pure steroid. In other words, $C_A(0)$ is the solubility of steroid A in polymer P. To calculate that solubility, we need to know the melting temperature of A, the enthalpy (or entropy) of fusion of A and the activity coefficient of A in P. Michaels calculates this activity coefficient using the Flory-Huggins theory of polymer solutions with interaction (Flory) parameter χ estimated from Hildebrand's regular-solution theory:

$$\chi = \frac{v_A(\delta_A - \delta_P)^2}{RT} \tag{2}$$

where v_A is the molar volume of (liquid) A and δ is the solubility parameter estimated by a group-contribution method.

Because the solubility of A in P is very small, the activity coefficient is calculated at infinite dilution. When the phase-equilibrium expression for $C_A(0)$ is substituted into the flux equation [Equation (1)],

$$\ln\,[\hat{J}_A \ell \cdot \exp(1+\chi)] = \frac{-\Delta h_f}{R}\left(\frac{1}{T} - \frac{1}{T_m}\right) + \ln \rho_A D \tag{3a}$$

$$= \frac{-\Delta s_f}{R}\left(\frac{T_m}{T} - 1\right) + \ln \rho_A D \tag{3b}$$

where Δh_f and Δs_f are, respectively, the molar enthalpy and entropy of fusion; T_m is the melting temperature and ρ_A is the mass density of (liquid) A. The derivation of Eq. (3b) is given in Ref. (1).

For correlation of data, Michaels used Eq. (3b) rather than Eq. (3a) because, for the steroids of interest here, the entropy of fusion is more nearly the same than the enthalpy of fusion [average $\Delta s_f = 16.7 \pm 3.5$ cal/mole, K].

Figure 2 shows (schematically) measured flux data for a variety of steroids in a variety of polymers. The data are plotted as suggested by Equation (3b); here 310 is body temperature: 273 + 37 = 310K. Each line is for a polymer characterized by its solubility parameter. We obtain straight lines with slopes remarkably close to that predicted by the entropy of fusion; for a fixed polymer, we expect that the product $\rho_A D$ is nearly constant.

With Figure 2, it is possible to make reliable estimates of the flux that we may expect for a particular steroid in a particular polymer with a particular thickness. For a given steroid, the desired flux is fixed by the drug's manufacturer. The correlation shown in Figure 2 provided significant help to the designers of the drug-delivery device. Help was provided in the usual way: by reducing the amount of experimental work needed to find the optimum design. Following a limited number of experimental studies that measured flux for a few steroids in a few polymers, the molecular-thermodynamic correlation in Figure 2 enabled the designers to choose the required thickness for a particular polymer for attaining the desired flux for a particular steroid.

This example indicates how well-known concepts in molecular thermodynamics can be used for developing a new product. However, molecular thermodynamics by itself is not sufficient. To obtain a useful result, molecular thermodynamics must be combined with another science; in this case, the theory of diffusion

A similar but much more sophisticated example is provided by another example: design of a polymer blend for creating a new material with desired mechanical properties.

Design of a Polymer Blend

To obtain desired mechanical, thermal and optical properties in polymeric products, it is useful to mix suitable polymers that differ in chemical and physical characteristics. But, unfortunately, for polymers the entropy of mixing (per unit mass) is so small that most polymers do not mix; they are incompatible. Nevertheless, it is possible to make polymer mixtures (called blends) that are stable, although they are not at equilibrium. Such blends are made by dissolving two (or more) polymers in a common volatile solvent and then rapidly removing the solvent by flash evaporation. While the solvent is present, the polymers are in a homogeneous solution. As the solvent evaporates, the polymers tend to segregate, i.e., to demix by spinodal decomposition. However, because polymer diffusion is slow and because polymer molecules become entangled as solvent disappears, complete demixing does not occur. The final stable polymer blend is a micro-heterogeneous mixture where the scale of heterogeneity is small, in the range of 100 - 1000 Angstroms. (In a mixture of compatible polymers the scale of heterogeneity is much smaller than that for a blend). To the naked eye, even to an optical microscope, a blend appears to be totally homogeneous but heterogeneity is evident to more powerful instruments like an electron microscope. The mechanical, thermal and optical properties of a polymer blend depend strongly on the nature and extent of heterogeneity, in short, on its morphology. At present, polymer blends are made mostly by empirical (Edisonian) procedures based on experience and trial and error. Can molecular-thermodynamic models contribute toward establishing a rational procedure for design of a polymer blend?

The answer, of course, is yes but the important word is "contribute". A molecular-

thermodynamic model by itself is not enough. However, when a molecular-thermodynamic model is combined with other, non-thermodynamic theoretical relations, a useful result can be obtained. Toward constructing a rational design method for non-equilibrium, micro-heterogeneous polymer blends, a molecular-thermodynamic model must interface first, with a theory for transport and second, and more difficult, a theory for describing the free energy of a non-equilibrium material with small spatial variations in composition, that is, composition gradients.

Such interfacing has been described by E. B. Nauman and co-workers at Rensselaer Polytechnic Institute (2, 4). To achieve practical results, a variety of simplifying assumptions must be made and, although the key equations are all analytic, the necessary calculations require numerical integrations.

The goal of Nauman's work was to obtain quantitative information on the extent (scale) of heterogeneity in a blend containing three different polymers. He achieved this goal for a relatively simple case where all three polymers have the same radius of gyration and where all three binary diffusion coefficients are identical. While Nauman's achievement is far from trivial, it is noteworthy that the theories he used are not new; indeed, in part, they are more than 50 years old. For describing the free energy of a microheterogeneous material, Nauman used the Landau-Ginzburg expansion first published about 40 years ago. For describing the Helmholtz energy of an equilibrium polymer mixture, he used the familiar Flory-Huggins equation. For a transport theory, he used a generalization of Fick's law; while that law goes back to the nineteenth century, its

modern multicomponent form dates back at least two generations. The only relatively new theoretical result in Nauman's work is an equation by de Gennes (1981) needed to evaluate a key coefficient in the Landau-Ginzburg expansion. The important achievement of Nauman is not development of new theory but courageous combination of several theories that have been available for many years.

For our purposes here, there is no need to go into details. To indicate in outline form the procedure required to apply a molecular-thermodynamic model toward rational product design, it is sufficient to look at the key equations that were used by Nauman and co-workers and to present a brief glance at some results.

We are concerned with a micro-heterogeneous mixture of polymers (after solvent removal) at a constant temperature and volume. We assume that there is no crystallinity and that the state of the mixture is rubbery, not glassy. The Helmholtz energy of mixing ΔA is given by

$$\Delta A = \int \Delta a \, d\check{r} \tag{4}$$

where $\check{r}$ indicates (three-dimensional) position and integration is over the entire volume of the mixture. Here Δa is the specific Helmholtz energy of mixing, i.e., the Helmholtz energy of mixing per unit volume.

In a micro-heterogeneous mixture, Δa depends on $\check{r}$. We expect Δa to depend on all local volume fractions $\phi_i(\check{r})$ and on all local spatial concentration gradients $\nabla\phi_i(\check{r})$ where i indicates a component. In a mixture containing M components, i = 1, 2, 3, ...M.

The essential contribution of Landau-Ginzburg theory is to provide a method for calculating the properties of a mixture with concentration gradients. Landau-Ginzburg theory uses a second-order expansion (i.e., a Taylor series) to relate Δa for a micro-heterogeneous mixture to Δa for a homogeneous mixture of the same overall composition, at the same temperature and volume.

$$\Delta a\,[\phi_i(\check{r}), \nabla\phi_i(\check{r})] = \Delta a\,[\phi_i(\check{r})] + \frac{1}{2}\sum_i^M \sum_j^M K_{ij}\,\nabla\phi_i(\check{r})\nabla\phi_j(\check{r}) \tag{5}$$

The first term on the right side is the specific Helmholtz energy of mixing for a homogeneous mixture (gradients are zero) whose composition is given by $\phi_i(\check{r})$, etc.

Subscripts i and j stand for components. Coefficient K_{ij} is the second derivative of $\Delta a\,[\phi_i(\check{r})]$ with respect to gradient $\nabla\phi_i(\check{r})$ and gradient $\nabla\phi_j(\check{r})$; . Calculation of K_{ij} is discussed by de Gennes (3). It depends primarily on the polymer's radius of gyration.

In this Taylor expansion, the first derivative vanishes because of symmetry. This symmetry follows from the mathematical properties of a Taylor expansion for a constant-density system. When Δa is plotted against the order parameter (in this case, the composition gradient), the plot is a symmetric parabola with a minimum when the order parameter is zero.

For $\Delta a\,[\phi_i(\check{r})]$, we use the classic multicomponent Flory-Huggins theory

$$\Delta a\,[\phi_i(\check{r})] = \rho kT\left[\sum \frac{\phi_i(\check{r})}{m_i}\ln\phi_i(\check{r}) + \frac{1}{2}\sum_i^M \sum_j^M \chi_{ij}\phi_i(\check{r})\phi_j(\check{r})\right] \tag{6}$$

where ρ is the (constant) number density of polymer segments, k is Boltzmann's constant, T is absolute temperature and m_i is the number of segments in polymer molecule i. The binary Flory parameter χ_{ij} is for the ij pair; it is determined from equilibrium experiments or, perhaps, estimated from solubility parameters or group contributions. When $i = j$, $\chi_{ii} = \chi_{jj} = 0$.

The goal of Nauman's calculations is to obtain the composition profile $\phi_i(\check{r})$ because that determines morphology. For example, if the composition profile is given by a sinusoidal function, the period of that function determines the domain size, while the amplitude indicates how much the composition of one domain differs from that of its adjacent domain. The composition profile depends on time because polymer molecules diffuse in the mixture until, because of entanglement, diffusion stops.

Diffusion is described by the multicomponent form of Fick's law; for component i in a system containing M components, flux $\hat{J}_i(\check{r}_i)$ is given by

$$\hat{J}_i(\check{r}) = -\sum_{j=1}^{M-1} \frac{D_{ij}}{kT} \nabla [\mu_j(\check{r}) - \mu_M(\check{r})] \tag{7}$$

where D_{ij} is a diffusion coefficient and μ_i is the chemical potential of component i. That chemical potential is obtained from functional differention according to

$$\mu_i(\check{r}) = \frac{\delta A}{\delta \rho_i(\check{r})} \tag{8}$$

where ρ_i is the number density of component i [$\rho_i(\check{r})$ is the composition profile in density units.] Here A is the total Helmholtz energy of the mixture. (A is the sum of the

Helmholtz energies of the pure components and ΔA given by Eq. (4).]

In Eq. (7) the summation is for M-1 components because only M-1 diffusion equations are independent. The M'th diffusion equation is not independent because of the conservation equation

$$\sum_{i=1}^{M} \hat{J}_i(\check{r}) = 0 \tag{9}$$

Finally, we have the equation of continuity:

$$\frac{\delta \rho_i(\check{r})}{\delta t} = -\nabla \hat{J}_i(\check{r}) \tag{10}$$

where t is time.

Nauman defines a dimensionless time τ

$$\tau = \frac{t\,D}{R_g^2} \tag{11}$$

Further, Nauman assumes that all diffusion coefficients D_{ij} are equal and that radius of gyration R_g is the same for all polymers.

The numerical problem is to integrate Eq. (10) and thereby obtain the volume fraction profile $\phi_i(\check{r})$ as a function of time. As τ increases, this profile approaches an asymptote. For that asymptote, Nauman stops the integration when $\tau = 2000$.

Depending on Flory parameters χ_{12}, χ_{13}, χ_{23}, Naumann's calculations provide significantly different morphologies. Figure 3 shows (schematically) two representative asymptotic morphologies. These can be compared with experimental morphologies obtained by electron microscopy shown in Figure 4.

Polymer-blend morphology has a strong influence on mechanical properties. To

illustrate, Figure 5 shows Izod impact strength for two blends. The lower line is for a binary blend containing 77 wt% polystyrene (PS), 23 wt% polyisobutylene (PB). The upper line is for a ternary blend containing 74 wt% PS 18 wt% PB and 8 wt% random copolymer containing 48 wt% PS and 52 wt% PB. Results are shown as a function of time because morphology depends on time following solvent removal. Here molding time refers to the time that the blend is kept at a constant high temperature where significant diffusion occurs. Following the molding time, the blend is cooled quickly, in effect, stopping all diffusion.

There is no simple theoretical way to relate mechanical properties to morphology; that relation is obtained from experimental experience. But once that experience is available, thermodynamic calculations can predict, or at least suggest, what blend compositions are most likely to give desired properties.

The Flory-Huggins equation can be used for blends of homopolymers or random copolymers but not for blends containing block copolymers. For such blends, molecular simulation must be used, as discussed by Nauman. Figure 6 shows simulations for a model system. The initial morphology is shown in part (a). As time passes, the particle size of the discontinuous (white) component grows and the block copolymer congregates at the periphery of the discontinuous phase. As morphology changes, so do mechanical (and other) properties. Using methods very briefly outlined here, morphology can often be predicted as a function of composition and time.

The calculations summarized here are not simple but, with powerful numerical

methods now available, they are within the grasp of enterprising chemical engineers who have daring, boldness and stamina and, perhaps, helpful support from a computer-oriented applied mathematician. The results obtained from these and similar calculations can provide valuable guidance toward formulation of polymer blends for specific applications.

For our purposes here, the essential message is that, for extending the boundaries of applied molecular thermodynamics, our primary need is not for new models but rather for the courage to use existing molecular-thermodynamic models in conjunction with other existing theoretical tools that go beyond thermodynamics. Nauman's example uses a combination of models (Flory-Huggins, Landau-Ginzburg, Fick) that have been in the literature for many years. His impressive contribution lies in showing that, when existing models are coupled together, they can provide useful results toward guiding and minimizing experimental efforts for development of new chemical products.

Precipitation of Proteins from Aqueous Solutions

While application to product design is a major new frontier for molecular thermodynamics, the more traditional application to process design also presents new challenges. To illustrate, my final example concerns molecular thermodynamics for biotechnology: precipitation of proteins from aqueous solution with salts. Such precipitation is common in biotechnology. For rational design, we want the phase diagram for an aqueous protein solution where temperature is plotted against protein concentration. Ultimately, we want such diagrams for multicomponent protein solutions. For our purposes here, however, we confine attention to a single-protein solution (5,7).

For protein solutions, the phase diagram is qualitatively different from that for ordinary fluids because the nature of intermolecular forces in such solutions is different from that for simple substances, e.g., argon (6,8).

How do we calculate the essential phase diagram for argon? We do so by writing an equation of state for fluid argon (gas or liquid) and another for solid argon. We are not here concerned with a complete quantitative description but with a semi-quantitative representation that captures, not the details, but the essentials. Toward that end, we use two simple van der Waals theories, one for the fluid phases and one for the crystalline solid.

For the fluid phases, we use the hard-sphere Carnahan-Starling equation with an attractive perturbation based on the Sutherland potential where the attractive part is given by an inverse power function of reduced intermolecular (center-to-center) distance r/σ; here σ is the protein's diameter. The exponent in that function is given by parameter n. Figure 7 shows a plot of the Sutherland potential. For argon-like substances, we expect London dispersion forces to dominate, giving an exponent n near 6. As n rises, the range of attraction decreases and, as we shall see in a moment, this decrease has a profound effect on the phase diagram. While n is near 6 for argon-like substances, it tends to be larger for proteins where the (reduced) range of attraction is less than that for simple nonpolar substances.

For solid argon with coordination number z we also use a hard-sphere expression perturbed by an attractive contribution based on the same Sutherland potential with the

same n.

Figure 8 shows a calculated phase diagram for argon. Proceeding from left to right, we first have the gas, then the two-phase vapor-liquid dome, then the freezing line and finally, the melting line. We are all familiar with this sort of diagram as found in a typical thermodynamics text. The top of the vapor-liquid dome is the well-known critical point.

For a protein solution, we make similar calculations. However, in this case the Sutherland potential represents a potential of mean force. For argon, the potential represents intermolecular forces between two argon atoms separated by a vacuum. For proteins in solution, the potential of mean force represents intermolecular forces between two protein molecules in a continuous solvent medium. In this case, the characteristic energy parameter ϵ/k depends not only on the nature of the protein but also on the nature of the solvent. For protein precipitation, the solvent may be an aqueous solution of salt or polymer.

From the equation of state for the fluid, we can show that the two-phase dome is independent of exponent n if we reduce temperature T not by ϵ/k but by T_c, the calculated critical temperature.

Figure 9 shows the effect of exponent n on the phase diagram. As shown by several authors, as the reduced range of attraction falls (in other words, as n rises), the freezing line moves to the left. At sufficiently large n, we obtain the unexpected result that the freezing line lies <u>above</u> the two-phase dome.

In the upper part of Figure 9, the left side of the diagram shows the dilute protein solution (analogous to the gas phase) while the right side represents the crystal. In the lower part of Figure 9, the two-phase dome shows the saturated dilute solution on the left in equilibrium with the saturated concentrated solution on the right. The top of the two-phase dome shows the upper critical solution (consolute) point.

From colloid theory, we expect that, as we add salt or polymer to a dilute solution at constant temperature, T_c rises or T/T_c falls.

Theoretical and experimental studies have shown that, for large particles (colloids or globular proteins), attractive forces are more short-ranged than those for simple molecules like argon. In other words, for large particles (charged or not), exponent n is larger than that for small molecules (9, 11).

On Figure 9, consider a dilute solution at a reduced temperature above the freezing line for say, $n = 6.4$. As T/T_c falls, we intersect the freezing line and, provided we attain equilibrium, a crystal appears. However, because of kinetic resistance, in practice we may not obtain a crystal; upon further decrease in T/T_c, we may intersect the liquid-liquid coexistence curve. Because the kinetic resistance for forming a second liquid phase is much less than that for forming a crystal, in practice, we may obtain not the equilibrium crystal but a second highly concentrated protein solution.

In Figure 9, for large n, the liquid-liquid region is metastable with respect to the liquid-solid region. However, because of kinetic factors, in practice, the metastable region may be remarkably stable.

Figure 10 compares calculated and experimental results for lysozyme. In this calculation, n = 8.2 and z = 8 (10). Protein diameter σ is obtained from x-ray diffraction data for the protein crystal and T_c can be obtained from experimental osmotic-second-virial coefficients for a dilute aqueous protein solution containing a specific salt at a specific ionic strength at a specific pH.

In presenting this example, all details have been omitted to illustrate the essential message: Molecular-thermodynamic analysis is useful for application to new phenomena encountered in process engineering. While the model briefly discussed here correctly reproduces only the essentials, refinements are likely to achieve good quantitative agreement. Extension to multi-protein systems is not trivial but not prohibitive; indeed, extension to aqueous binary protein mixtures has already been achieved. The example shown here illustrates the happy fact that simple models--in many cases, old models--are often applicable to help solve new problems in chemical technology.

Conclusion

The examples shown here were chosen to illustrate two propositions.

First, to assist product development, chemical-engineering thermodynamics must interface with other scientific areas, notably mass transfer. Chemical engineering thermodynamics by itself is often insufficient. For effective application, chemical engineering thermodynamics must be part of a larger whole, a contributing member of a team. For product development, our motto should be: chemical engineering thermodynamics in context.

Second, chemical engineering thermodynamics is often most useful when it is directed at developing models for new situations, that is, for situations where our quantitative understanding is seriously inadequate. Pioneering molecular thermodynamics is concerned not with improvements where primary understanding has already been achieved, but with shedding light on situations where, as yet, we know very little. Much of current research falls into this category but regrettably, much of that research, while brilliant, neglects to show applicability.

Finally, the examples I have shown use simple theories that are not new. No doubt new theories are required for some phenomena of rising interest in chemical engineering but for many practical problems, old theories are sufficient, provided that they are used with courage and imagination.

I started with a short quotation from Einstein. Let me now close with a short quotation from the German playwright Bertold Brecht, author of the well-known "Three-Penny Opera". In that play, there is a penetrating line

"Erst kommt das Fressen; dann kommt die Moral."

Loosely translated, this means "First fill your belly, then think about philosophy."

After almost 50 years of activity in applied thermodynamics, I have learned to appreciate Brecht's sound, realistic advice. I therefore urge all in this audience: do the best work in thermodynamics that you possibly can and enjoy it thoroughly. But don't lose sight of the goal. Thermodynamics comes second. First comes chemical engineering.

Acknowledgments

For financial support, the author is grateful to the Director, Office of Energy Research, Office of Basic Energy Sciences, Chemical Sciences Division of the US Department of Energy; to the National Science Foundation; and to the Donors of the Petroleum Research Fund administered by the American Chemical Society. For helpful discussions, the author thanks J. Z. Wu and especially E. B. Nauman, who also kindly provided Figures 5 and 6.

References

First Example

[1] A.S. Michaels et al, AIChE Journal, 21 (1975) 1073.

Second Example

[2] E.B. Nauman and D.Q. He, Polymer, 35 (1994) 2243.
[3] P.G. de Gennes, J. Chem. Phys., 72 (1981) 4756.
[4] E.B. Nauman, Chemical Engineering Dept., Rensselaer Polytechnic Institute, Troy, NY 12180-3590, personal communications.

Third Example

[5] H. Mahavedan and C.K. Hall, AIChE J., 38 (1992) 573.
[6] M. Muschol and F. Rosenberger, J. Chem. Phys., 107 (1997) 1953.
[7] F.W. Tavares and S.I. Sandler, AIChE J., 43 (1997) 218.
[8] D. Rosenbaum and C.F. Zukoski, J. Crystal Growth, 169 (1996) 752.
[9] D. Rosenbaum et al, Phys. Rev. Letters, 76 (1996) 150.
[10] J. Ulrich, Diplomarbeit for Univ. of Karlsruhe, performed at Univ. of California, Berkeley (1997).
[11] J. Israelachvili, Intermolecular and Surface Forces, Second Edition, Academic Press, London, 1992.

Nomenclature

A	Helmholtz energy
a	Helmholtz energy per unit volume
C	concentration
D	diffusion coefficient
Δh_f	enthalpy of fusion
$\hat{J}$	flux
K	coefficient in the Landau-Ginzburg expansion
k	Boltzmann's constant
ℓ	thickness
n	exponent in potential function
m	no. of segments in polymer molecule
$\check{r}$	three-dimensional position
R	gas constant
R_g	radius of gyration
Δs_f	entropy of fusion
T	temperature
T_c	critical temperature
T_m	melting temperature
t	time
v	molar volume
z	coordination number
δ	solubility parameter in Eq. (2)
ϵ	potential-energy parameter
ρ	mass density or number density
χ	Flory parameter
σ	diameter
ϕ	volume fraction
τ	dimensionless time
μ	chemical potential

Figure Captions FPE 8818

1. Drug-Delivery Device: Steroid Diffuses Through the Wall of a Polymer. Wall Thickness is ℓ.

2. Correlation of Flux Data for Steroid i Diffusing Through a Wall of Polymer P. Solubility Parameters δ Estimated from Group Contributions.

3. Illustrative Calculated Morphologies in a Mixture of Three Polymers. These Morphologies are Obtained from Calculated Density (Concentration) Profiles for Polymers 1, 2 and 3.

4. Experimental Electron Micrographs for Two Ternary Mixtures of Polystyrene (PS), Polymethylmethacrylate (PMMA), Polybutadiene (PB) (a) PS 50%, PMMA 40%, PB 10% (b) PS 40%, PMMA 50%, PB 10%

5. Izod Impact Strength Vs. Time for a Binary Blend of Polystyrene (PS) Polybutadiene (PB) and a Ternary Blend of PS/PB/SB Random Copolymer. PS (M_n = 82,000; M_w = 202,000); PB(M_n = 130,000; M_w = 320,000); SB Random Copolymer (48% PS; M_n = 140,000; M_w = 420,000)

6. Morphologies at Difference Times for Mixtures with Low Block Concentrations (6%). Monte-Carlo Seconds (MCS): (a) 0, (b) 10, (c) 100, (d) 10^3, (e) 10^4, (f) 10^5. Gray and White Represent Homopolymers. Black represents Block Copolymer.

7. Sutherland Potential for Two Particles with Diameter σ. As Exponent n Rises, the Reduced Range of Attraction Declines.

8. Calculated Phase Diagram for a Simple Substance Showing Vapor-Liquid and Liquid-Solid Equilibria

9. Calculated Phase Diagrams for Different Exponent n. As n Rises, the Liquid-Liquid Coexistence Curve Tends to Lie Below the Freezing Line.

10. Calculated and Experimental Phase Diagram for Lysozyme in Aqueous Sodium Chloride Solutions

CONTROLLED DRUG DELIVERY. DIFFUSION OF A STEROID THROUGH A POLYMERIC CONTAINER

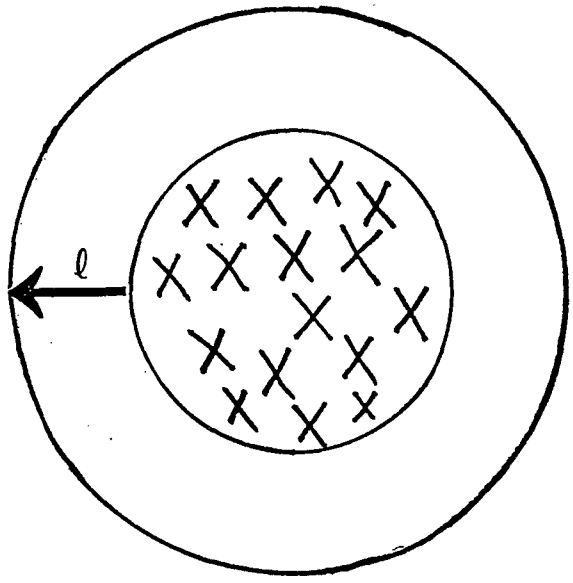

X = STEROID

$$\text{FLUX } \hat{J} = D \left[\frac{c(o) - c(\ell)}{\ell} \right]$$

c = STEROID CONCENTRATION IN POLYMER
$c(\ell) = o$
c(o) = SOLUBILITY OF STEROID IN POLYMER
D = DIFFUSIVITY
ℓ = THICKNESS OF POLYMER CONTAINER

Figure 1

CORRELATION OF FLUX DATA
(MICHAELS ET AL, 1975)

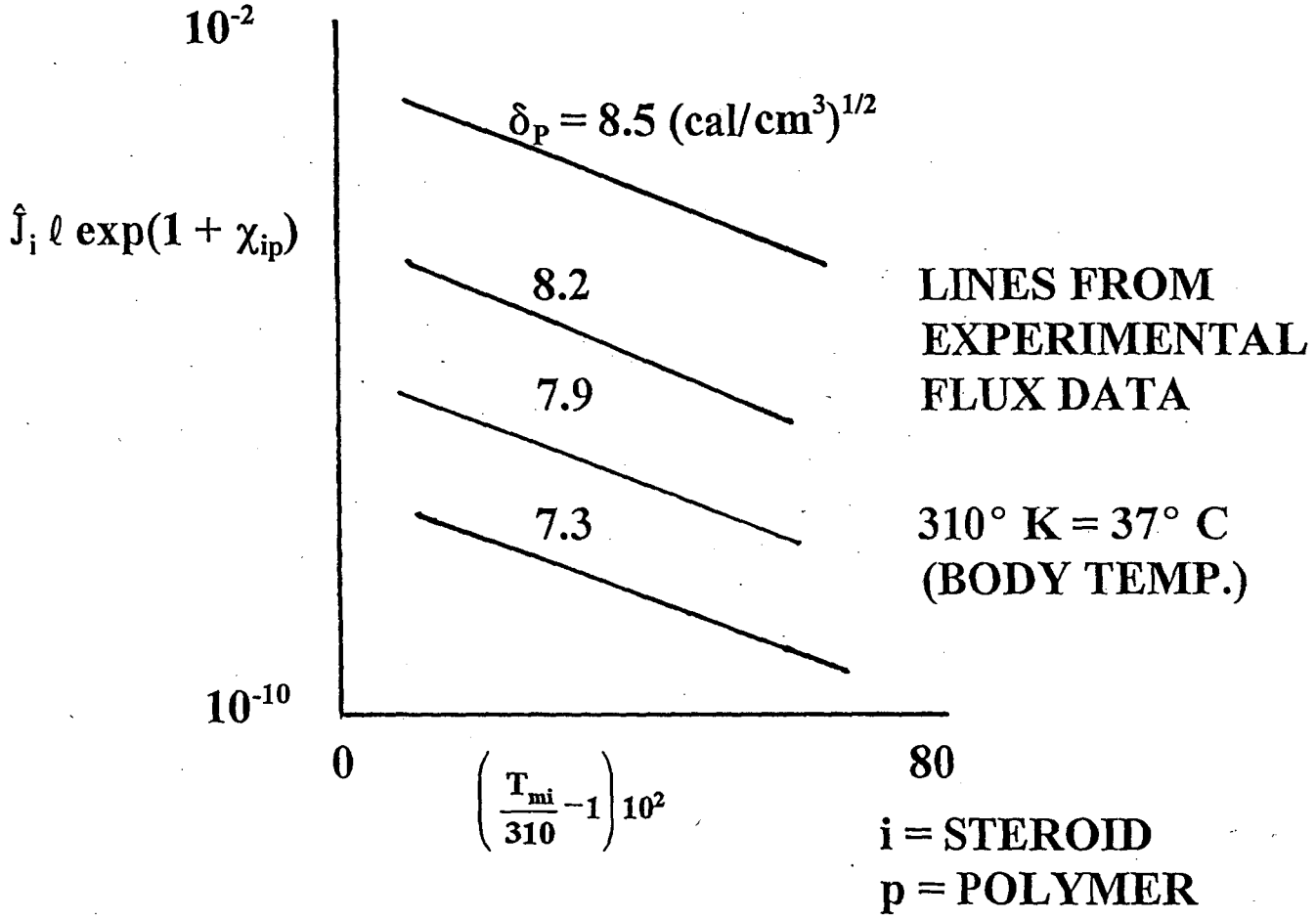

STEROIDS: PROGESTERONE, TESTOSTERONE, ESTRADIOL, CORTISOL, ESTRIOL, PREDNISOLONE AND OTHERS.

POLYMERS: POLYDIMETHYL SILOXANE, POLYETHYLENE, POLY(CO-ETHYLENE-VINYL ACETATE) POLY(CO-POLYTETRAMETHYLENE ETHER GLYCOL-DIPHENYLMETHANE DI-ISOCYANATE) AND OTHERS.

Figure 2

TWO TYPES OF CALCULATED MORPHOLOGY FOR A TERNARY POLYMER BLEND (SCHEMATIC)

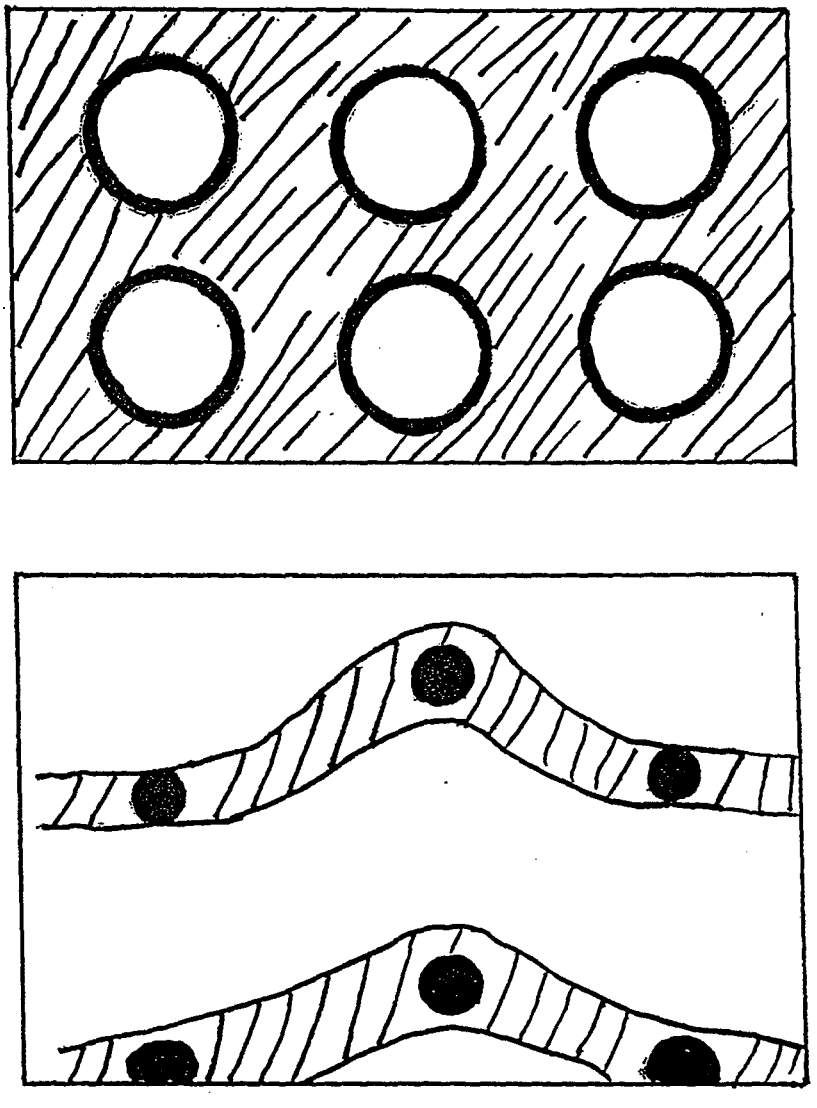

BLACK IS POLYMER 1
WHITE IS POLYMER 2
SHADED IS POLYMER 3

Figure 3

EXPERIMENTAL MORPHOLOGIES FROM ELECTRON MICROSCOPY

(a)

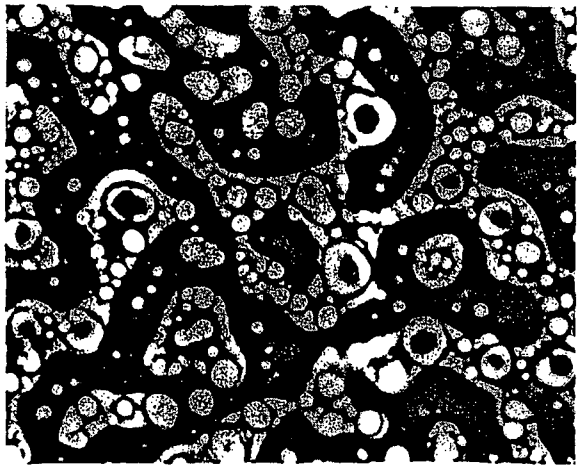

(b)

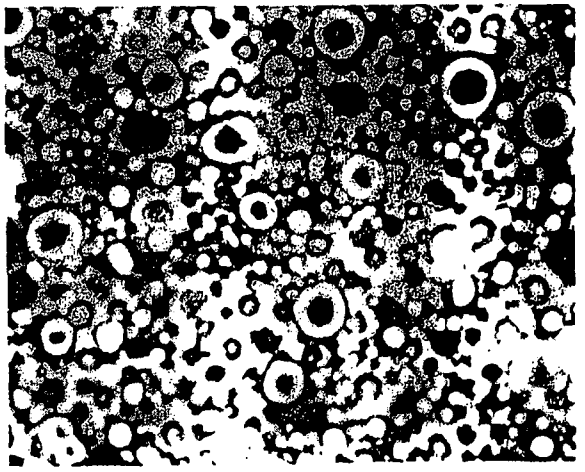

		%
(a)	PS	50
	PMMA	40
	PB	10

		%
(b)	PS	40
	PMMA	50
	PB	10

PS = POLYSTYRENE PMMA = POLYMETHYLMETHACRYLATE

PB = POLYBUTADIENE

Figure 4

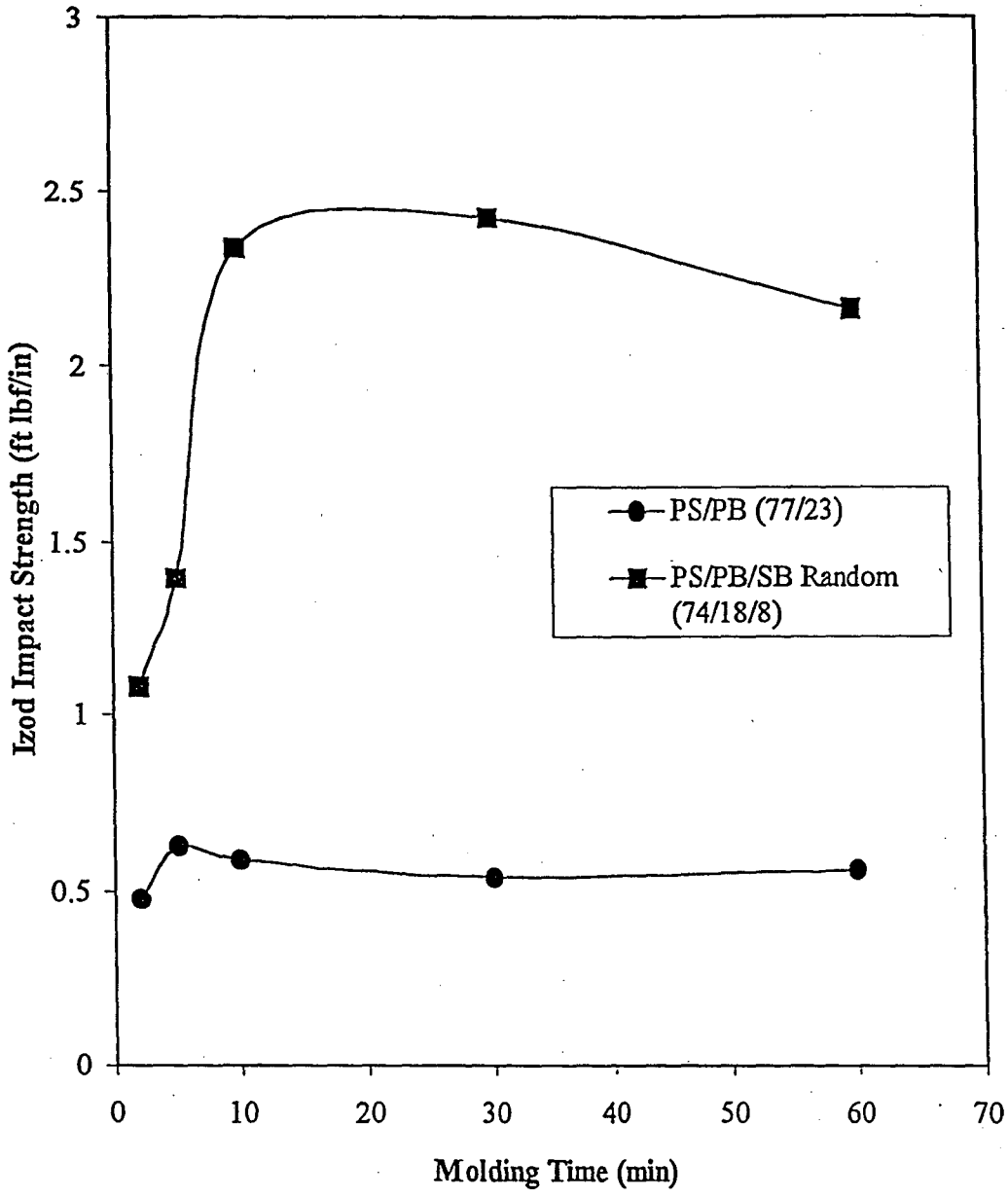

Izod Impact Strength vs. Time for a Binary Blend of PS/PB and a Ternary Blend of PS/PB/SB Random Copolymer. PS (Mn = 82000, Mw = 202000), PB (Mn = 130000, Mw = 320000); SB Random (48% PS, Mn = 140000, Mw = 420000)

Figure 5

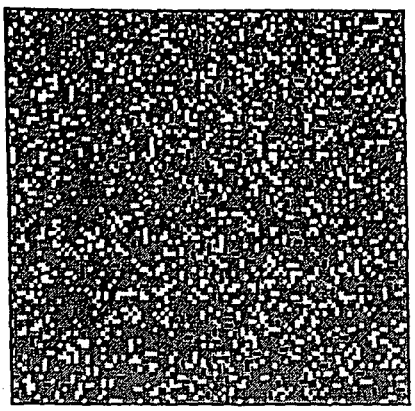

(a)

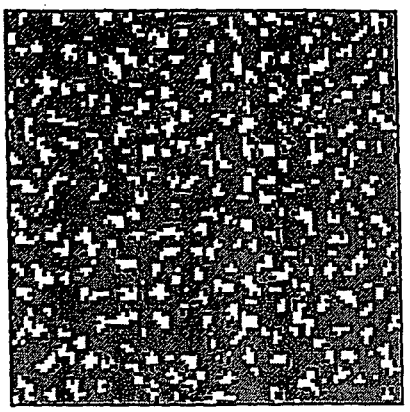

(b)

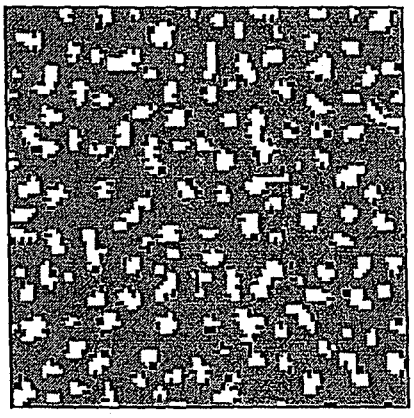

(c)

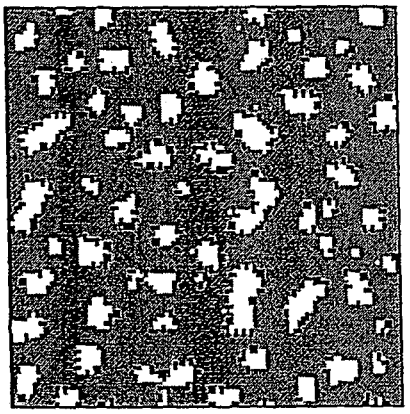

(d)

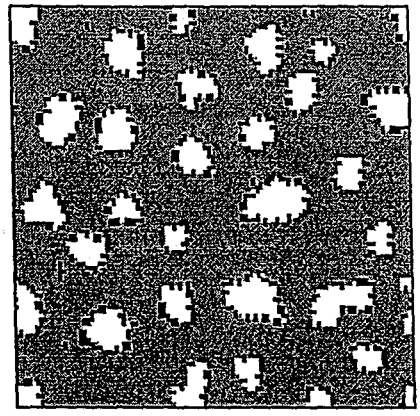

(e)

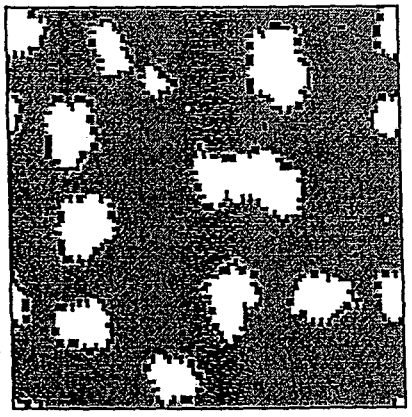

(f)

Morphologies at different times for the case with low block concentration (6%)
(a) 0 MCS, (b) 10 MCS, (c) 100 MCS, (d) 1000 MCS, (e) 10000 MCS, (f) 100000 MCS.
Gray and white represent the hompolymers while black represents the copolymer.
MCS = MONTE CARLO SECONDS

Figure 6

SUTHERLAND POTENTIAL. THE RANGE OF ATTRACTION DECREASES WITH RISING n

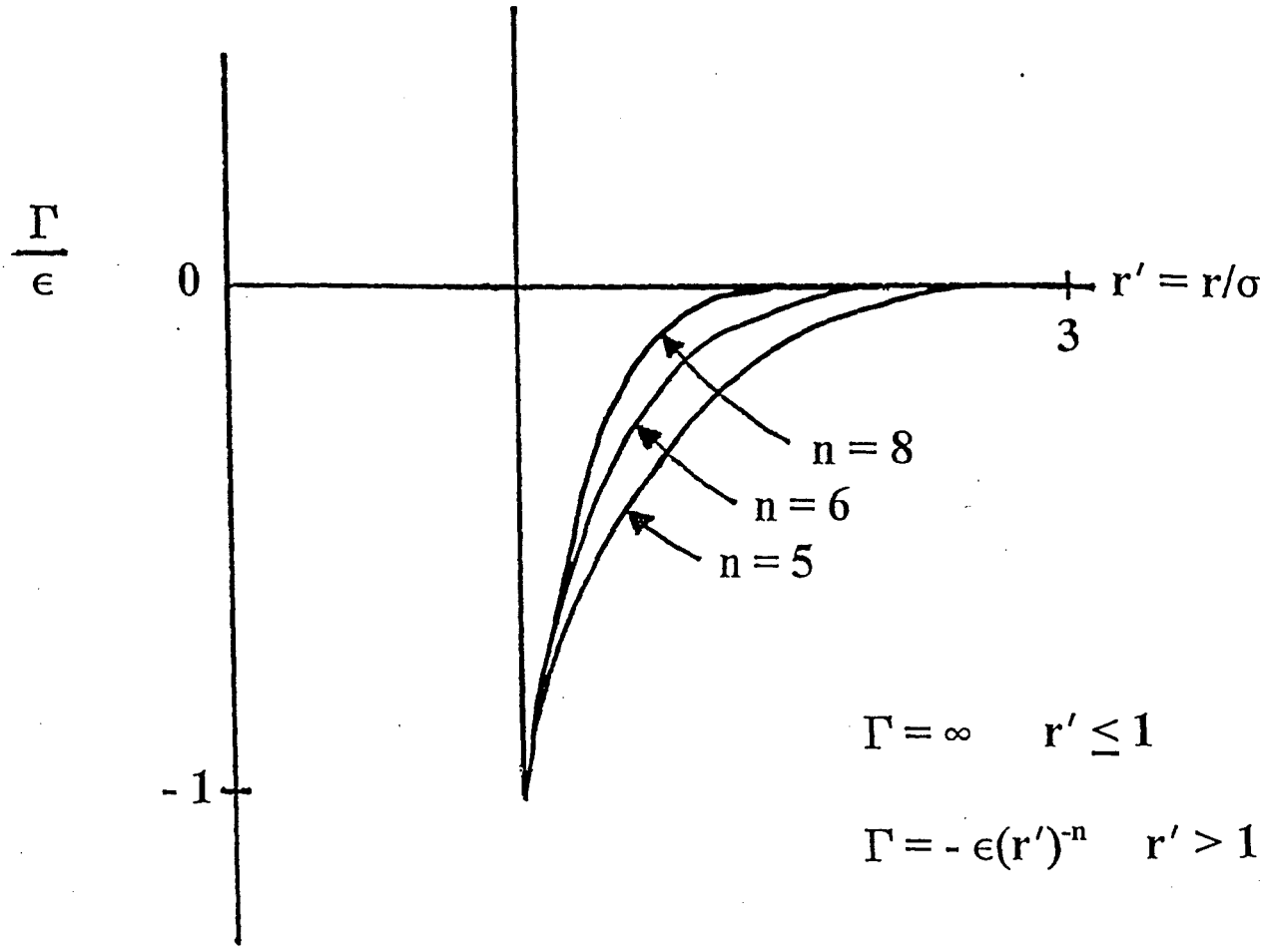

Figure 7

CALCULATED PHASE DIAGRAM (SCHEMATIC) FOR ARGON-LIKE FLUID

EXPONENT n = 6

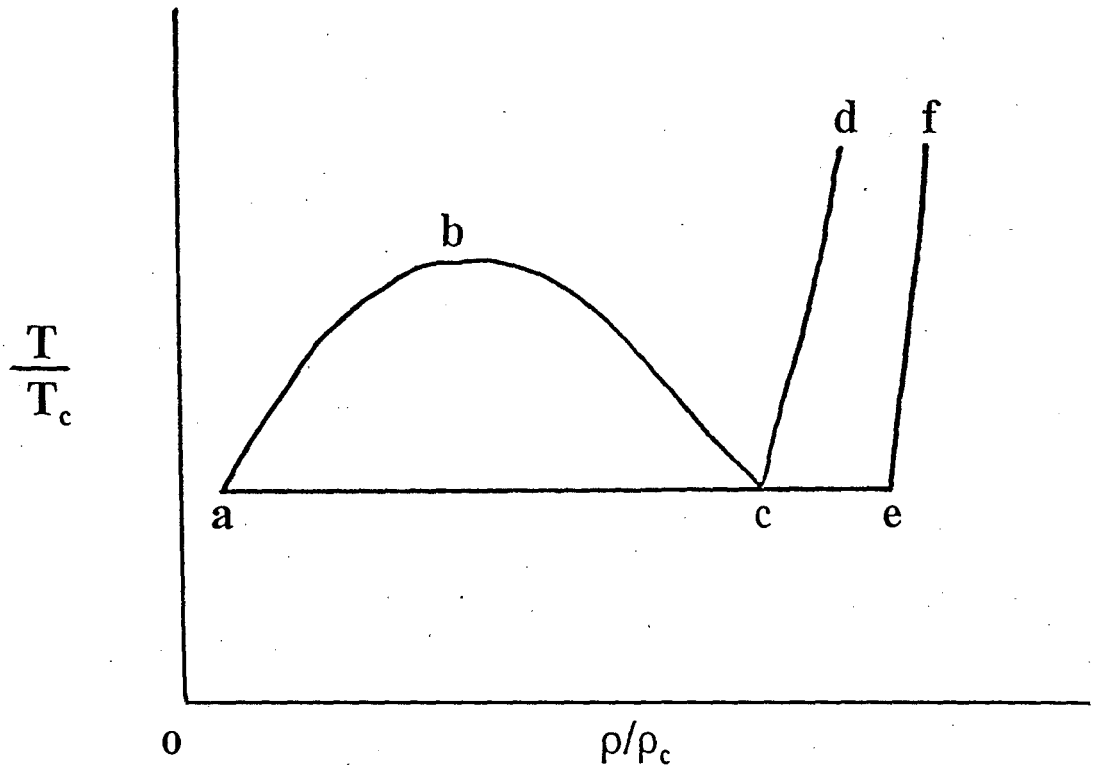

abc	FLUID-FLUID COEXISTENCE
cd	LIQUIDUS (FREEZING) LINE
ef	SOLIDUS (MELTING) LINE
ace	TRIPLE-POINT LINE

ρ = DENSITY
ρ_c = CRITICAL DENSITY
T_c = CRITICAL TEMPERATURE

Figure 8

CALCULATED PHASE DIAGRAMS (SCHEMATIC) FOR VARYING EXPONENT n

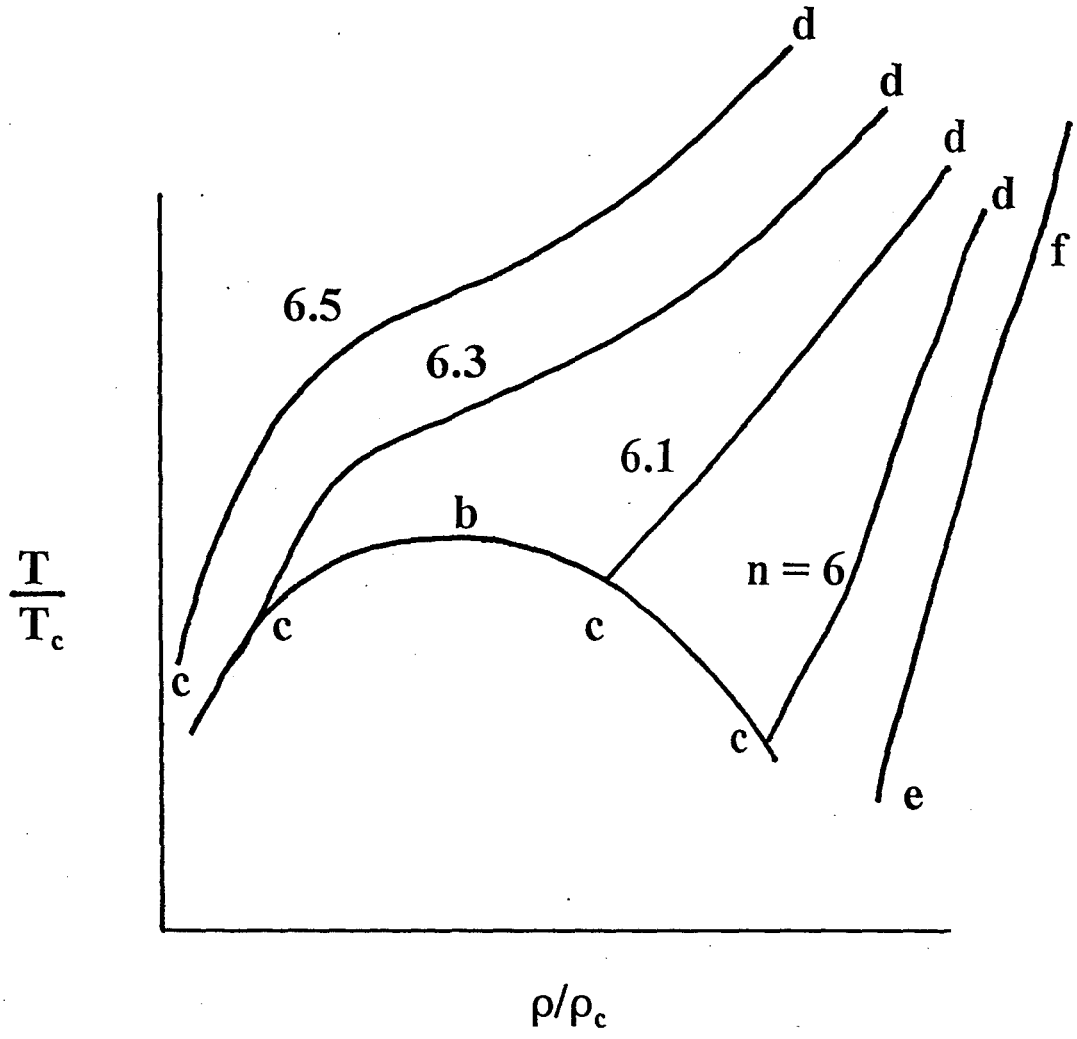

b IS THE FLUID-FLUID CRITICAL POINT. MELTING LINE ef CHANGES ONLY WEAKLY WITH n.

BUT

FREEZING LINE cd MOVES STRONGLY TO THE LEFT AS n INCREASES.

ON THESE COORDINATES, THE FLUID-FLUID COEXISTENCE LINE DOES NOT CHANGE WITH n.

Figure 9

CALCULATED AND OBSERVED PHASE DIAGRAM FOR LYSOZYME IN AQUEOUS NaCl pH 4.5

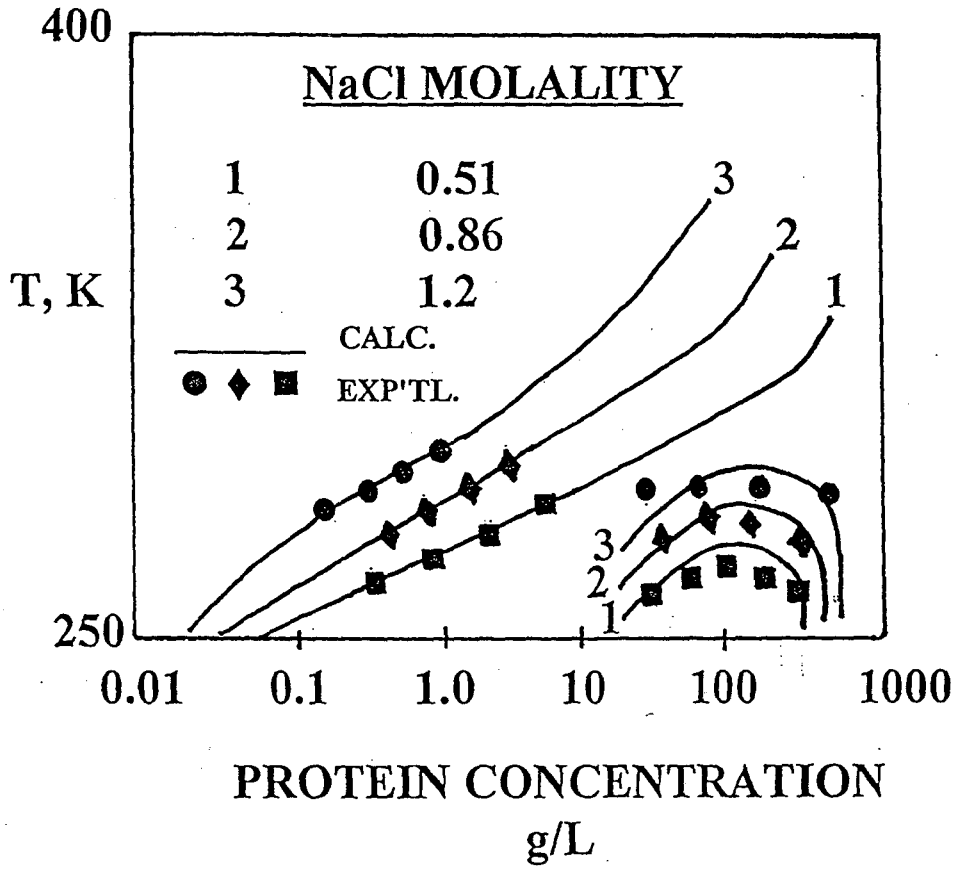

CALCULATIONS WITH n = 6.3 AND SOLID-PHASE COORDINATION NUMBER 12. σ = 34.4Å FROM CRYSTALLOGRAPHIC DATA.

ENERGY PARAMETER ϵ INCREASES WITH NaCl MOLALITY

Figure 10

Ernest Orlando Lawrence Berkeley National Laboratory
One Cyclotron Road | Berkeley, California 94720

Prepared for the U.S. Department of Energy under Contract No. DE-AC03-76SF00098